Supporting Information

Organic Monolayers on Si(211) for Triboelectricity Generation: Etching Optimization and Relationship between the Electrochemistry and Current Output

Carlos Hurtado,[a] Xin Lyu,[a] Stuart Ferrie,[a] Anton P. Le Brun,[b] Melanie MacGregor,[c] Simone Ciampi,[a,*]

[a]School of Molecular and Life Sciences, Curtin University, Bentley, Western Australia 6102, Australia

[b]Australian Centre for Neutron Scattering, Australian Nuclear Science and Technology Organization, Lucas Heights, New South Wales 2234, Australia

[c]Flinders Institute for Nanoscale Science and Technology, Flinders University, Bedford Park, South Australia 5042, Australia

Correspondence: simone.ciampi@curtin.edu.au

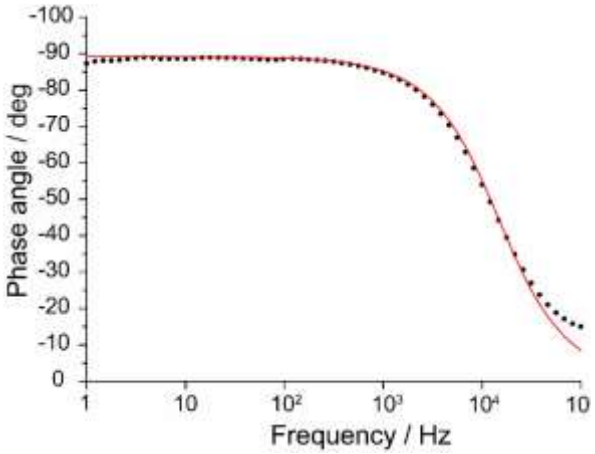

Figure S1. Representative EIS phase angle versus frequency plot for a **S-1** sample on Si(111). The E_{dc} was set to −0.5 V. Black dots are the experimental values, and the red line is the best fit (Chi-squared = 0.01). The equivalent circuit used in the fitting is shown in Section S2. Refined values of R_{film}, and C_{dl} where 6.2×10^6 Ω and 0.1×10^{-6} F respectively.

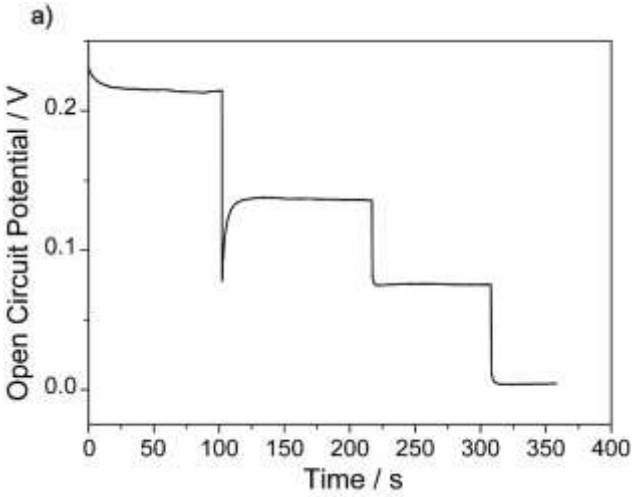

Figure S2. Progressive cathodic shift of the open circuit potential for a Si(111) **S-2** sample (photoanode) as a function of its illumination intensity. The electrode was irradiated with a red LED and progressively increasing the light intensity from dark (0 – 100 s), to 1.0 mW cm^{-2} (100 – 200 s), 1.7 mW cm^{-2} (200 – 300 s) and reaching 3.4 mW cm^{-2} (after 300 s).

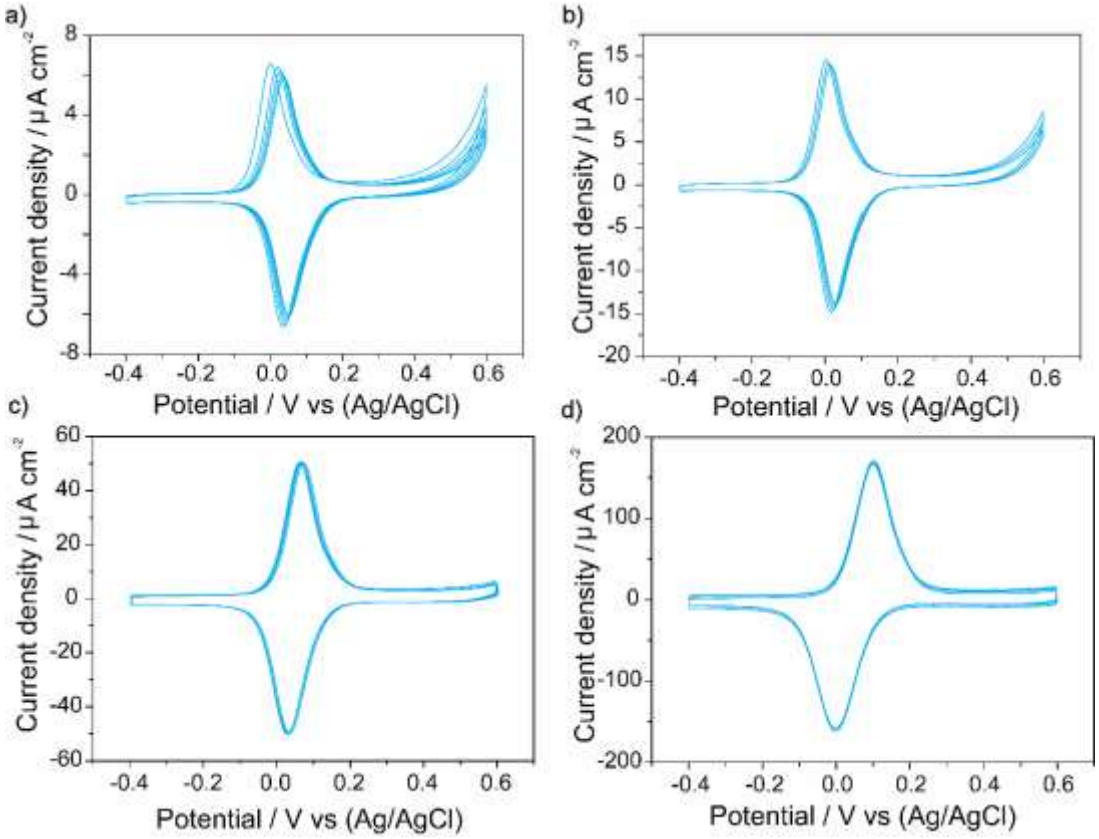

Figure S3. Representative cyclic voltammograms (CVs) for a **S-2** Si(111) photoanode. The electrode was illuminated at a light intensity of 1.7 mW cm^{-2}. The scan rate was (a) 50 mV/s, (b) 100 mV/s, (c) 500 mV/s and (d) 2000 mV/s.

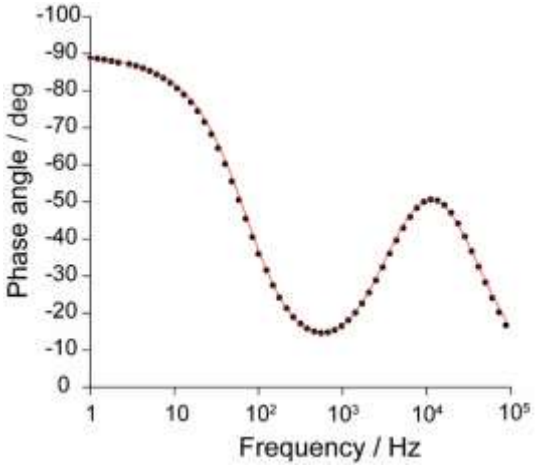

Figure S4. Representative EIS phase angle versus frequency plot for a **S-2** sample on Si(111). The E_{dc} was set to 0.1 V. The electrode was illuminated at a light intensity of 1.7 mW cm^{-2}. Black dots are the experimental values and the red line is the best fit (Chi-squared = 0.01). The equivalent circuit model used in the fitting is shown in Section S2. The refined k_{et} was $(3.6\pm1.4) \times 10^2$ s^{-1}.[1] Values of R_{et}, C_{ads}, and C_{dl} were 50.1 Ω, 4.2×10^{-5} F and 1.1×10^{-6} F, respectively. Capacitors were modelled as CPEs with power modifiers of 0.98 for C_{dl} and 0.99 for C_{ads}.

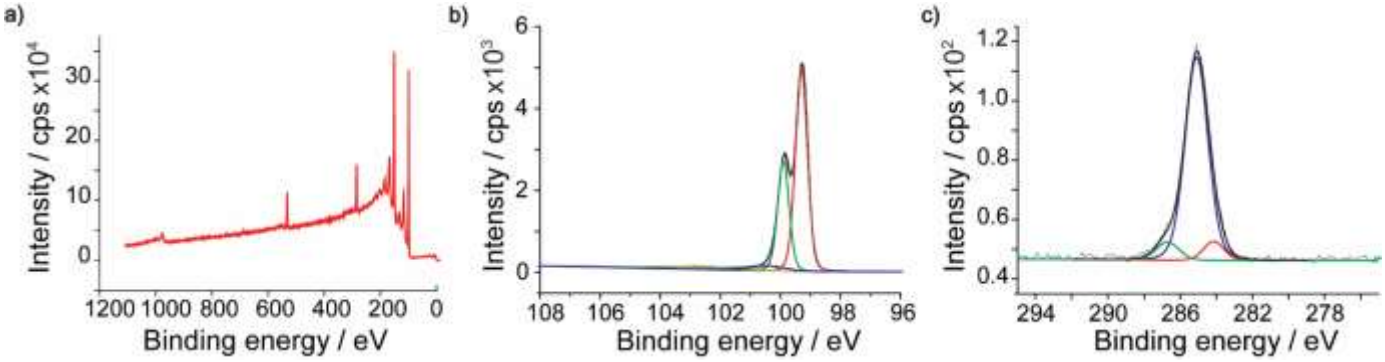

Figure S5. XPS spectra for **S-1** samples on Si(211). The etching time was 13 min [40% aqueous NH_4F under ambient light (0.2 mW cm^{-2})]. (a) XPS survey spectrum. (b) Narrow scan of the Si 2p region. The Si $2p_{3/2}$ peak was 99.5 eV. The high binding energy shoulder (0.40 eV higher than Si $2p_{1/2}$) is tentatively attributed to photoelectrons from Si−H species.[2] In the 101.5–104 eV region, photoelectrons from $Si^{(2)}$, $Si^{(3)}$ and $Si^{(4)}$ oxides merge into a single band. (c) Narrow scan of the C 1s region. The signal was deconvoluted into a main C–C peak (carbon bound to carbon) at 284.9 eV, a C–Si (carbon bound to silicon) at 284.0 eV, and a contribution at 286.9 eV ascribed to C≡C and/or C−OH.[3]

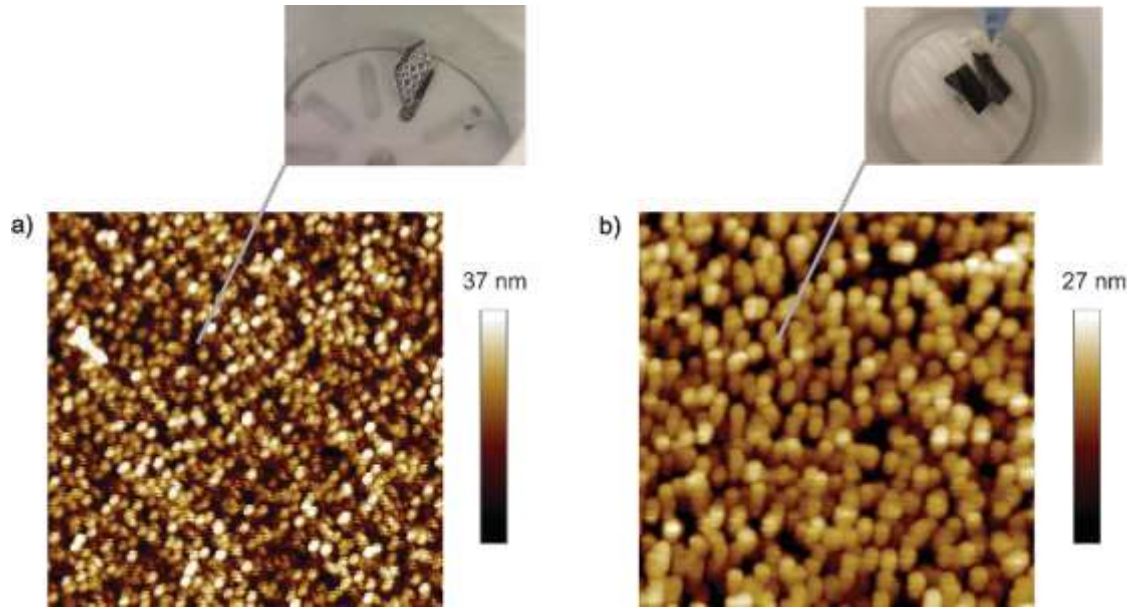

Figure S6. (a) AFM topography image of a **S-1** sample grafted on a Si(211) wafer etched for 13 min in aqueous 40% NH_4F under ambient light and in the absence of methanol. The sample roughness was 8.6 nm. The photograph shown in (a) above the AFM map shows the wafer while being etched. (b) AFM topography image of a representative **S-1** sample grafted on a Si(211) wafer etched for 13 min in a mixture of MeOH and 40% NH_4F (1:10) under ambient light. The sample roughness was 3.1 nm. The photograph shown in (b) above the AFM map shows the wafer while being etched.

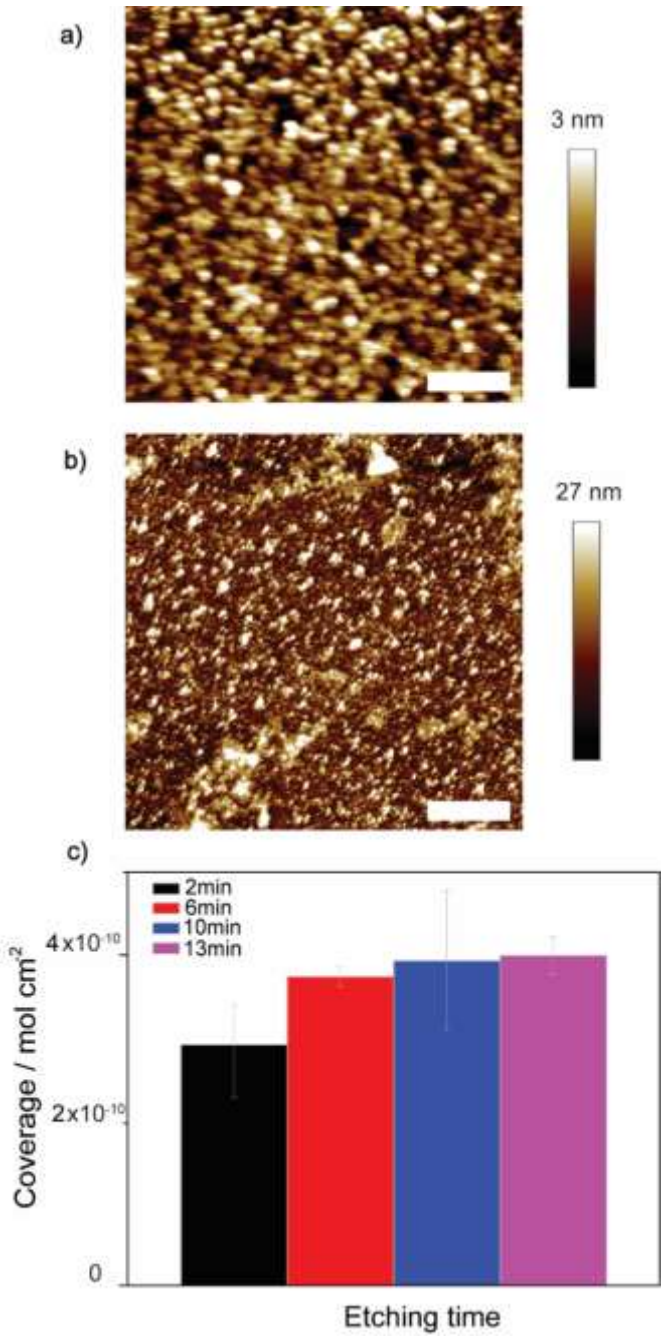

Figure S7. (a) AFM topography image of a representative **S-1** sample on Si(211). The wafer was etched for 2 min in a mixture of MeOH and 40% NH_4F (1:10), under ambient light (0.2 mW cm^{-2}). The sample roughness was 1.0 nm. (b) AFM topography image of a representative **S-1** sample grafted on Si(211) etched for 13 min in a mixture of MeOH and 40% NH_4F (1:10) under ambient light. Roughness value for the sample shown in panel was 3.4 nm. (c) Bar plot showing the evolution of the ferrocene coverage for **S-2** samples prepared from the **S-1** samples of (a) and (b) as well as on samples prepared via intermediate etching times. The etching time is shown in figure, and the error bars represent the standard deviation from the mean coverage value.

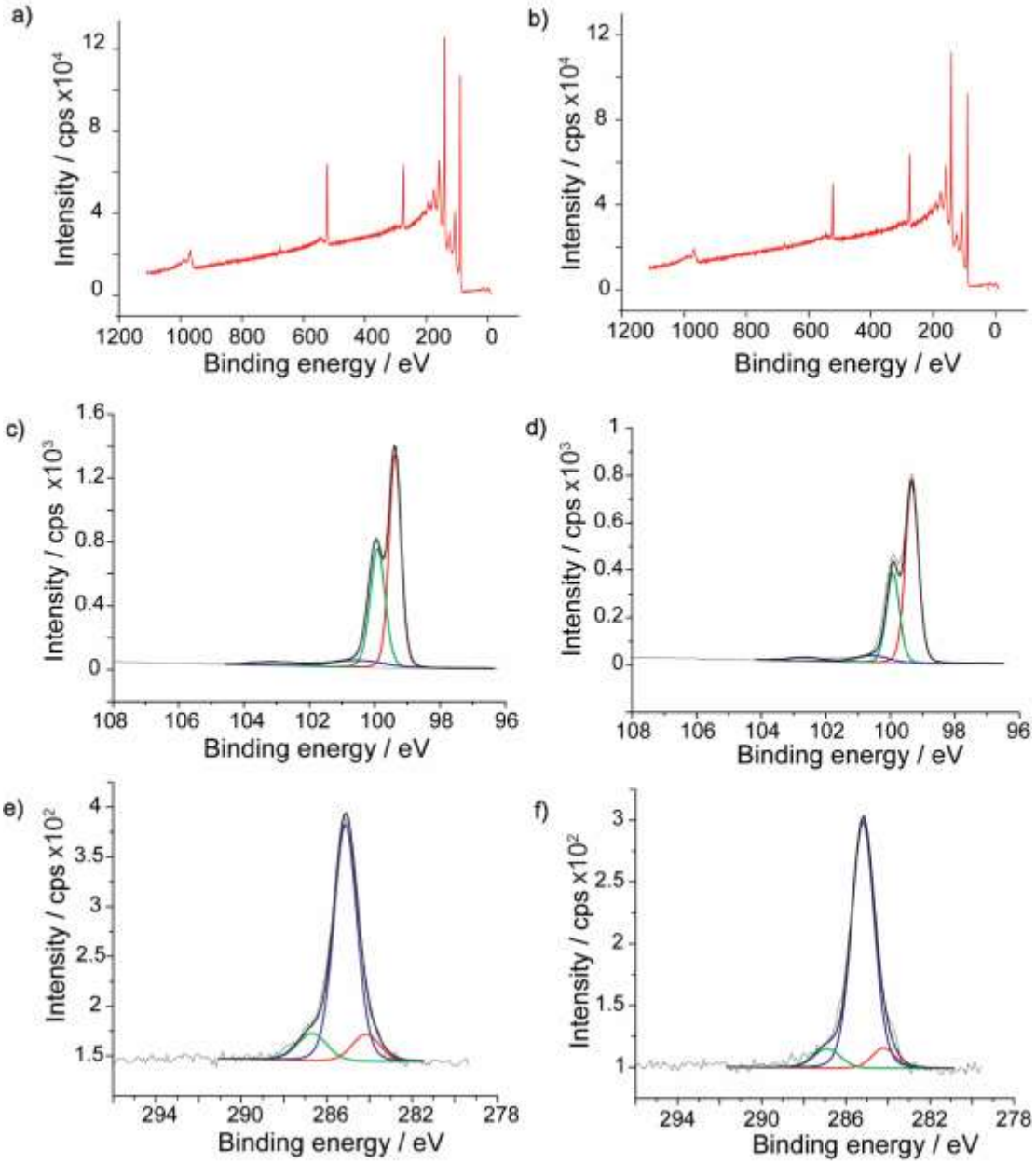

Figure S8. XPS data for **S-1** samples grafted on Si(211). The Si(211) substrates were etched for 2 min (a, c, e) and for 13 min (b, d, f), in a mixture of MeOH and 40% NH_4F (1:10) under ambient light (0.2 mW cm^{-2}). (a, b) XPS survey spectra. (c, d) Narrow scans of the Si 2p region. The Si $2p_{3/2}$ peak was at 99.5 eV. The high binding energy shoulder (0.40 eV from Si $2p_{1/2}$) is tentatively attributed to Si−H species.[2] In the 101.6–104 eV region, photoelectrons from $Si^{(2)}$ $Si^{(3)}$ and $Si^{(4)}$ oxides merge into a single band (2 min etch). Photoelectron from $Si^{(2)}$ and $Si^{(3)}$ and $Si^{(4)}$ oxides, are attributed to the signal at 101.5–103.7 eV (13 min etch). (e, f) Narrow scans of the C 1s region. The spectra were deconvoluted into a main C–C signal (carbon bound to carbon) at 284.9 eV, a C–Si (carbon bound to silicon) shifted at 284.0 eV, and a third contribution at 286.9 eV, ascribed to C≡C and/or C−OH.[3]

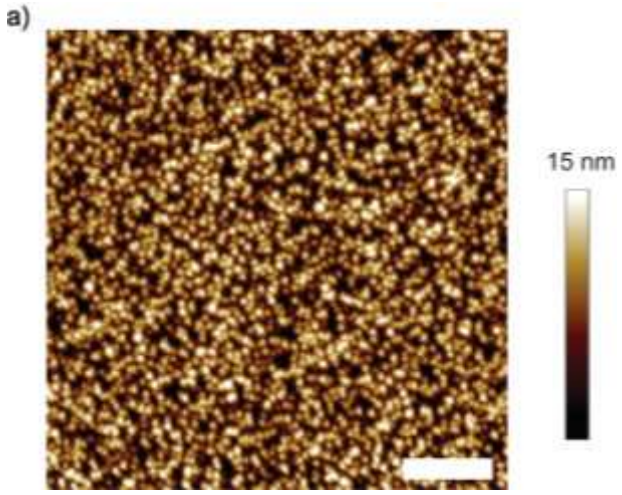

Figure S9. (a) AFM topography image of a representative **S-1** sample prepared on Si(211). The Si(211) substrate was etched for 13 min in a mixture of MeOH and 40% NH_4F (1:10) in dark. The roughness value for the sample shown in figure is 2.6 nm.

Table S1. Surface roughness (AFM data) for **S-1** samples on Si(211) as function of solvent, etchant, etching time and illumination levels

Solvent	Etching time (min)	Illumination ($mWcm^{-2}$)	Roughness (RMS, nm)
Aqueous 40% NH_4F	2	0.2	0.4 ± 0.1
MeOH 10%, 40% NH_4F (1:10, v/v)	2	0.2	0.9 ± 0.1
MeOH 10%, 40% NH_4F (1:10, v/v)	2	dark	0.7 ± 0.4
Aqueous 40% NH_4F	13	0.2	7.8 ± 3.2
MeOH 10%, 40% NH_4F (1:10, v/v)	13	0.2	3.2 ± 0.3
MeOH 10%, 40% NH_4F (1:10, v/v)	13	dark	2.6 ± 0.1

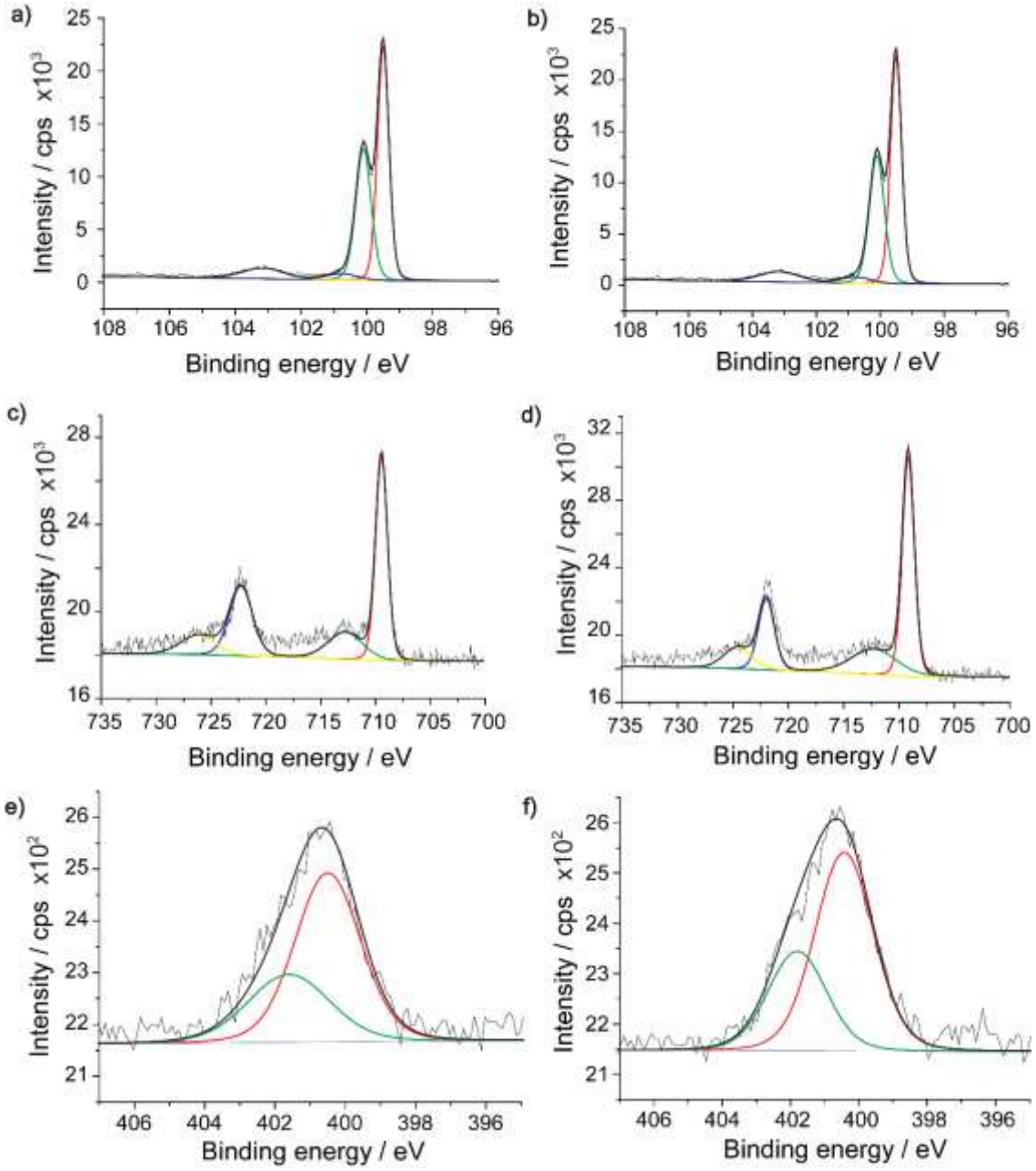

Figure S10. XPS data for **S-2** samples grafted on Si(111) (a, c, e), and on Si(211) (b, d, f). The Si(211) substrates were etched for 13 min in a mixture of MeOH and 40% NH_4F (1:10) under ambient light (0.2 mW cm^{-2}). (a, b) Narrow scans of the Si 2p region. The Si $2p_{3/2}$ peak was at 99.5 eV. The high binding energy shoulder (0.40 eV from the Si $2p_{1/2}$) is tentatively ascribed to Si−H species. In the 102–104 eV region, photoelectrons from $Si^{(2)}$, $Si^{(3)}$ and $Si^{(4)}$ oxides merge into a single band (2 min etch). Photoelectron from $Si^{(3)}$ and $Si^{(4)}$ oxides, are attributed to the signal at 102–104 eV (13 min etch). (c, d) Narrow scans of the Fe 2p region showing refined Fe $2p_{3/2}$ [708.6 eV for Fe(II)) and Fe $2p_{1/2}$ (721.5 eV for Fe(II)] spin–orbit-split signals. High binding energy shoulders are Fe(III) signals from ferricenium species. (e, f) Narrow scans of the N 1s region.

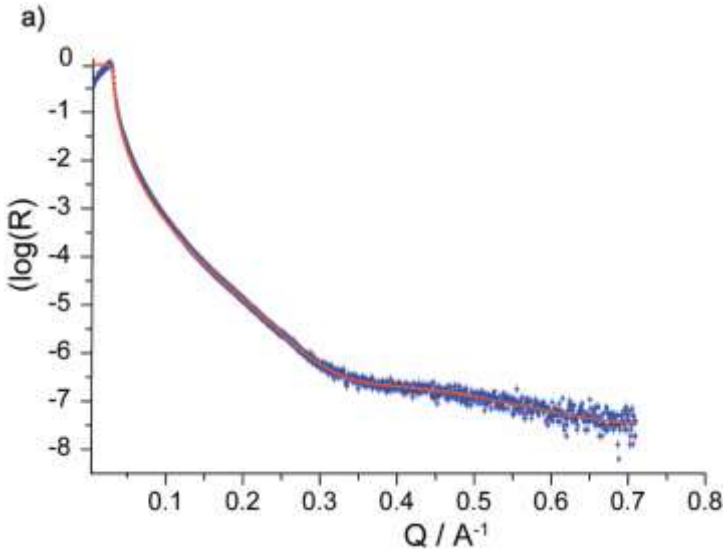

Figure S11. XRR profile for a **S-1** film on Si(111) surfaces. The refined model (red line) is shown over the experimental data (solid blue symbols, $\chi^2 = \sim 10$). The etching time was 13 min [40% aqueous NH_4F under ambient light (0.2 mW cm^{-2})]

Table S2. XRR Refined Structural Parameters for **S-1** films on Si(111) and Si(211)

	Si(111)	Si(211)
SLD ($Å^{-2}$)	1.3×10^{-5}	1.0×10^{-5}
Roughness monolayer–air interface (Å)	2.9	3.1
Roughness monolayer–silicon interface (Å)	3.2	8.2
Organic film thickness (Å)	9.5	10

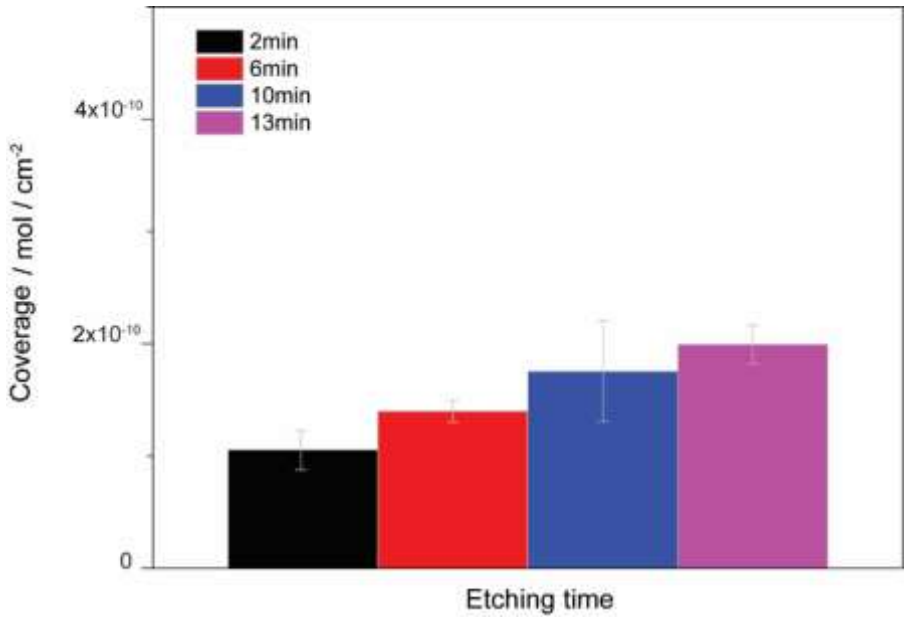

Figure S12. Evolution of the ferrocene surface coverage for **S-2** samples prepared on Si(211) with etching time. Si(211) substrates were etched in dark in a mixture of MeOH and 40% NH_4F (1:10). The etching time varied between 2 and 13 min and is specified in figure [(black) 2 min; (red) 6 min; (blue) 10 min; (pink) 13 min]. The error bar represents the standard deviation from the mean coverage value.

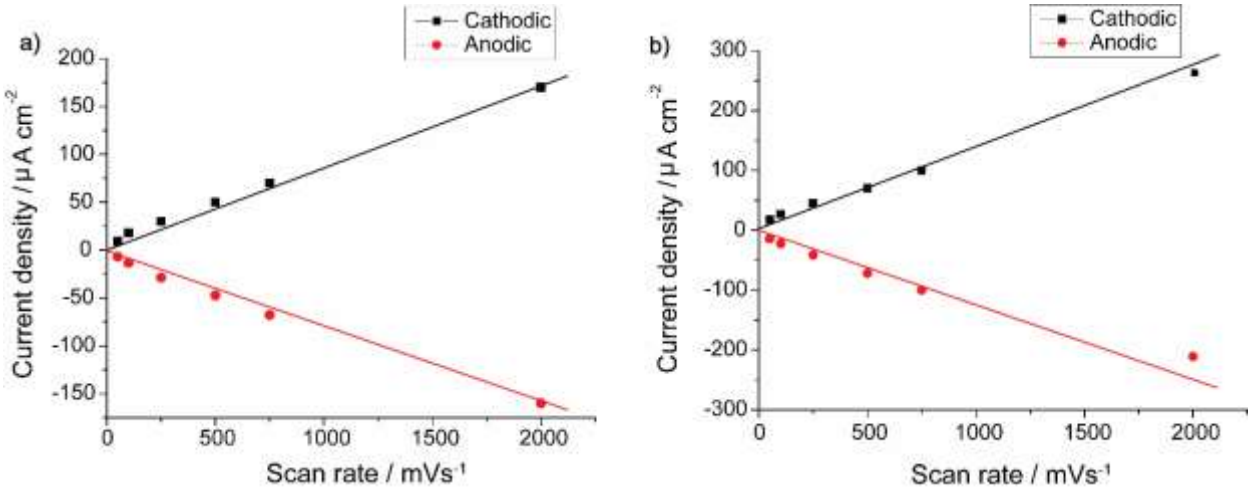

Figure S13. Cathodic and anodic peak heights (current density) as function of the voltage scan rate (mV/s) for **S-2** samples made on (a) Si(111) and (b) Si(211). The electrodes were illuminated at a light intensity of 1.7 mW cm^{-2}. Si(211) samples were etched in a mixture of MeOH and aqueous 40% NH_4F (1:10, v/v) in dark.

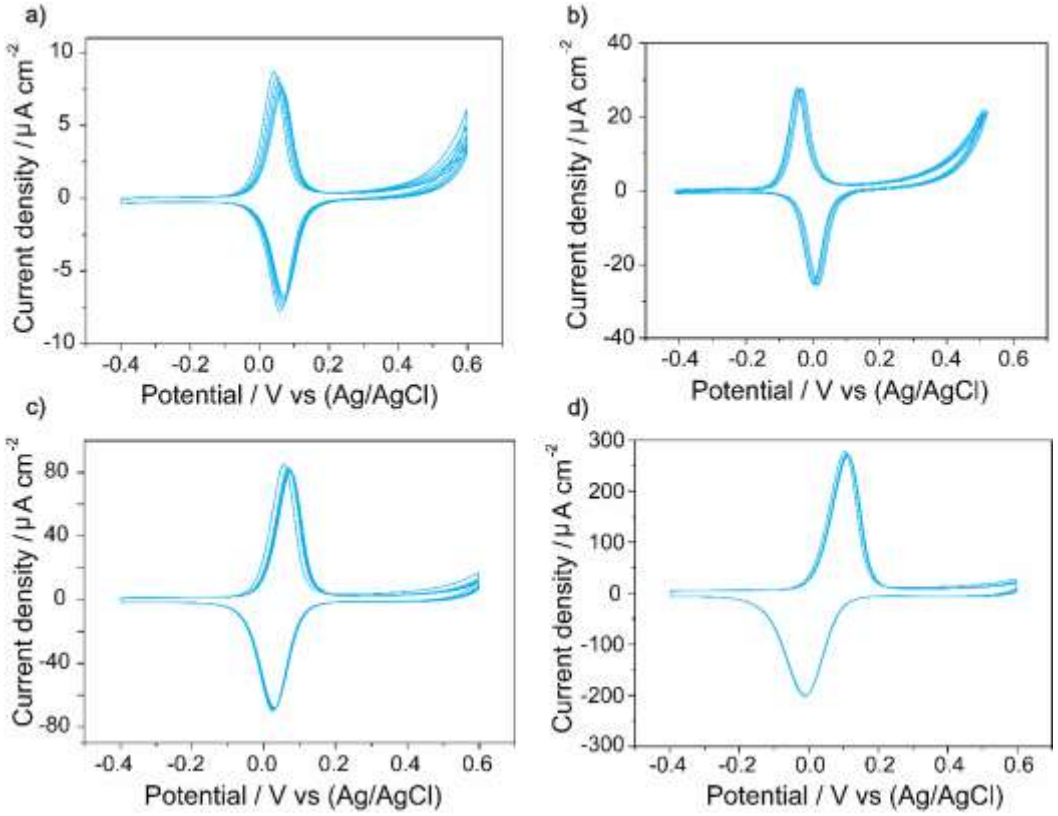

Figure S14. Representative cyclic voltammograms (CVs) for a **S-2** Si(211) photoanode. The electrode was illuminated at a light intensity of 1.7 mW cm^{-2}. The voltage scan rate was (a) 50 mV/s, (b) 100 mV/s, (c) 500 mV/s, and (d) 2000 mV/s. Samples were etched in a mixture of MeOH and aqueous 40% NH_4F (1:10, v/v) in dark.

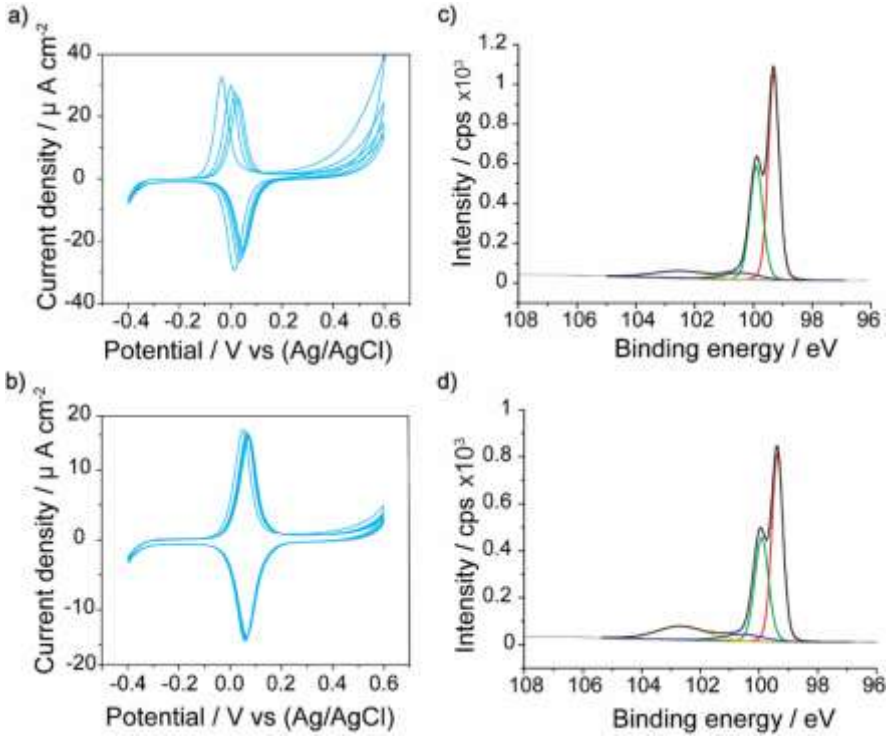

Figure S15. Representative CVs (100 mV/s, 1.0 M $HClO_4$) for **S-2** samples made on Si(211). The Si(211) substrate was etched in a mixture of MeOH and aqueous 40% NH_4F (1:10, v/v) in absence of light. The CVs in figure were recorded after either (a) 10 CV cycles or (b) 40 cycles. Cycles were in the −0.4 to 0.6 V range (100 mV/s, 1.0 M $HClO_4$). The electrodes were illuminated at a light intensity of 1.7 mW cm^{-2}. (c, d) XPS high-resolution Si 2p spectra for the samples analyzed by CVs in (a, b). A broad 100–104 eV signal is the result of photoelectrons from $Si^{(1)}$, $Si^{(2)}$, $Si^{(3)}$and $Si^{(4)}$ oxides.

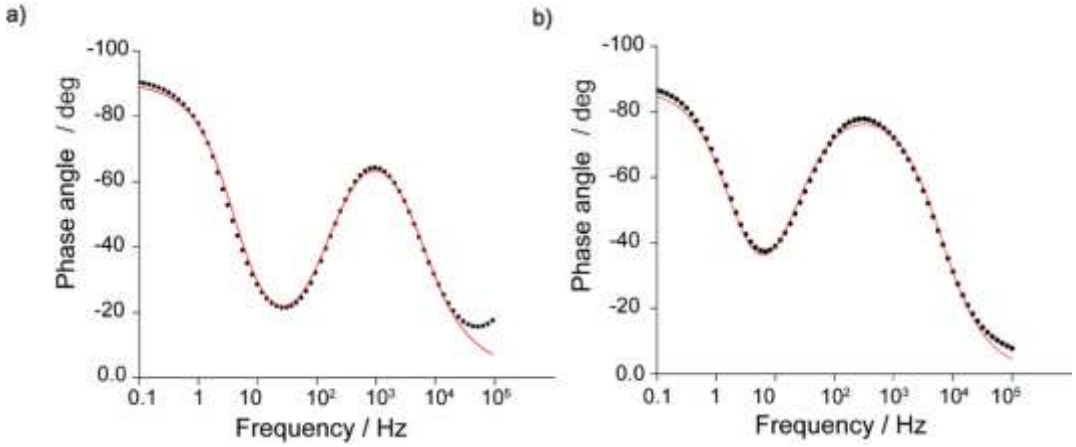

Figure S16. Representative EIS phase angle versus frequency plots for **S-2** samples on Si(211). Samples were anodically damaged by means of 10 and 40 cycles ((a) and (b) respectively) prior to the EIS experiments. The E_{dc} was set to 0.1 V. Black dots are the experimental values and the red lines the best fits. The equivalent circuit used in the fitting is shown in Section S2. Refined values of R_{et}, C_{ads}, and C_{dl} were 696.2 Ω, 5.5×10^{-5} F and 2.7×10^{-6} F for samples subjected to 10 CV cycles, and 7170 Ω, 1.2×10^{-5} F and 1.8×10^{-6} F for samples subjected to 40 cycles (yielding k_{et} of 12.9 s^{-1} and 5.9 s^{-1} respectively). Experimental data are solid points and the fits solid lines ((a) Chi-squared = 0.01, (b) Chi-squared = 0.02)). The substrate was Si(211) etched in a mixture of MeOH and aqueous 40% NH_4F (1:10, v/v) in dark.

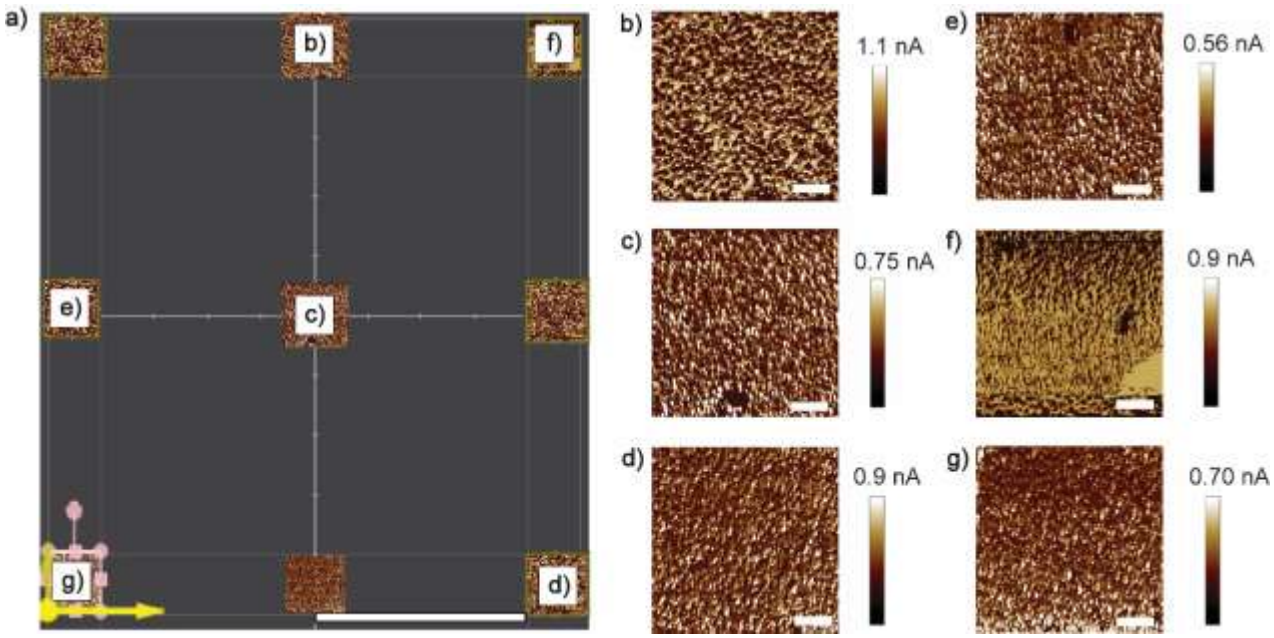

Figure S17. (a) Location of nine separate sampling regions across a Si(211) **S-1** surface. The horizontal scale bar is 2.5 mm, and the size of the AFM micrographs, indicating the actual sampling locations, is not up to scale. (b–g) Representative C-AFM maps for **S-1** Si(211) samples etched for 13 min in 1:10 v/v MeOH/NH_4F 40% while shielded from ambient light. Horizontal scale bars in (b–g) are 1 μm. The mean current output value for the different locations were (b) 241 pA, (c) 347 pA, (d) 293 pA, (e) 429 pA, (f) 371 pA, and (g) 434 pA.

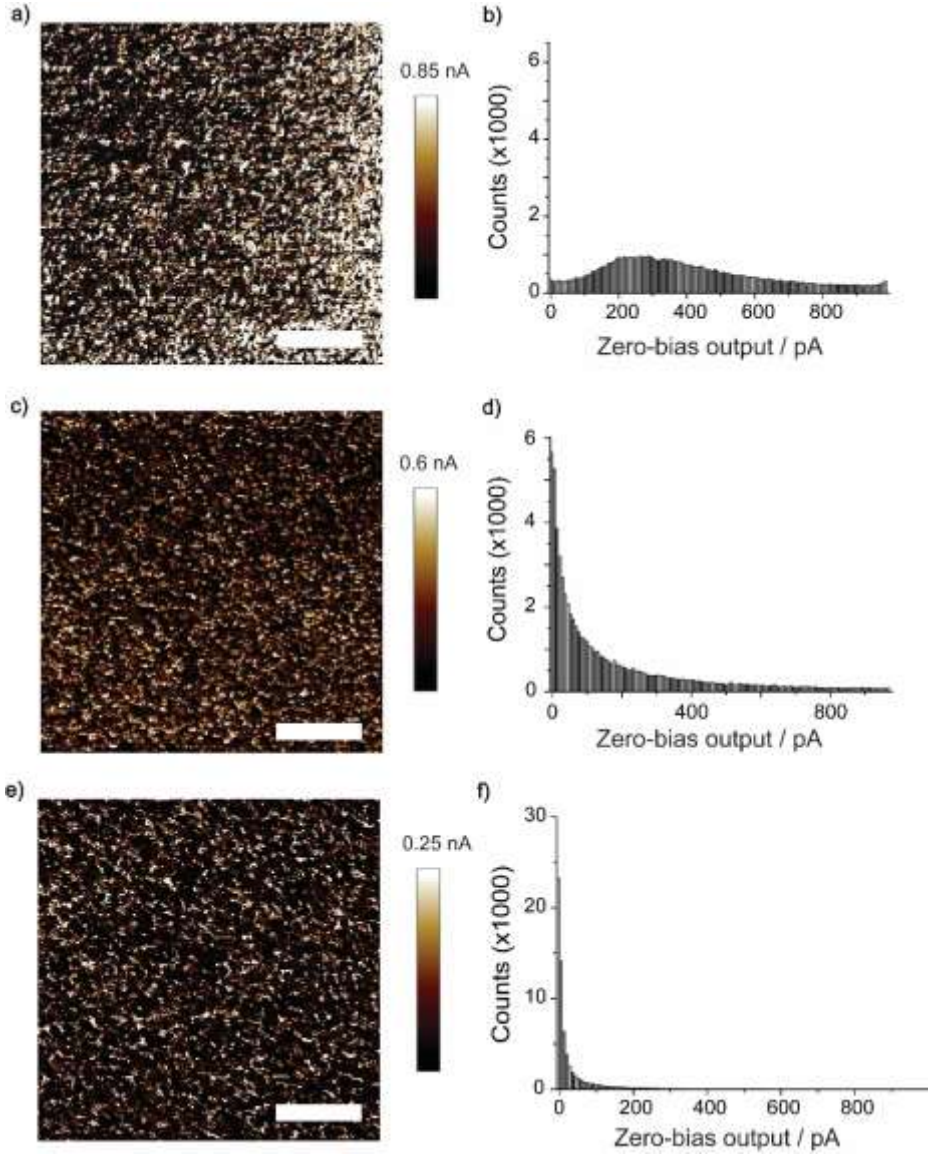

Figure S18. Zero-bias C-AFM maps for **S-1** samples etched under dark for 13 min in a mixture of MeOH and aqueous 40% NH_4F (1:10, v/v). Panels (a, c, e) are current maps recorded after 1 (mean of current output value of 352 pA), 2 (mean of current output value of 187 pA) and 3 (mean of current output value of 47 pA) successive scan cycles under 50 nN of normal force. Panels (b, d, f) show histograms of the current output in the C-AFM maps. The histograms' y–axis counts indicate the number of pixels (sample locations) of a given current magnitude, with a total of ~65k pixels making up a C-AFM map. Horizontal scale bars in panels (a, c, e) are 1 μm.

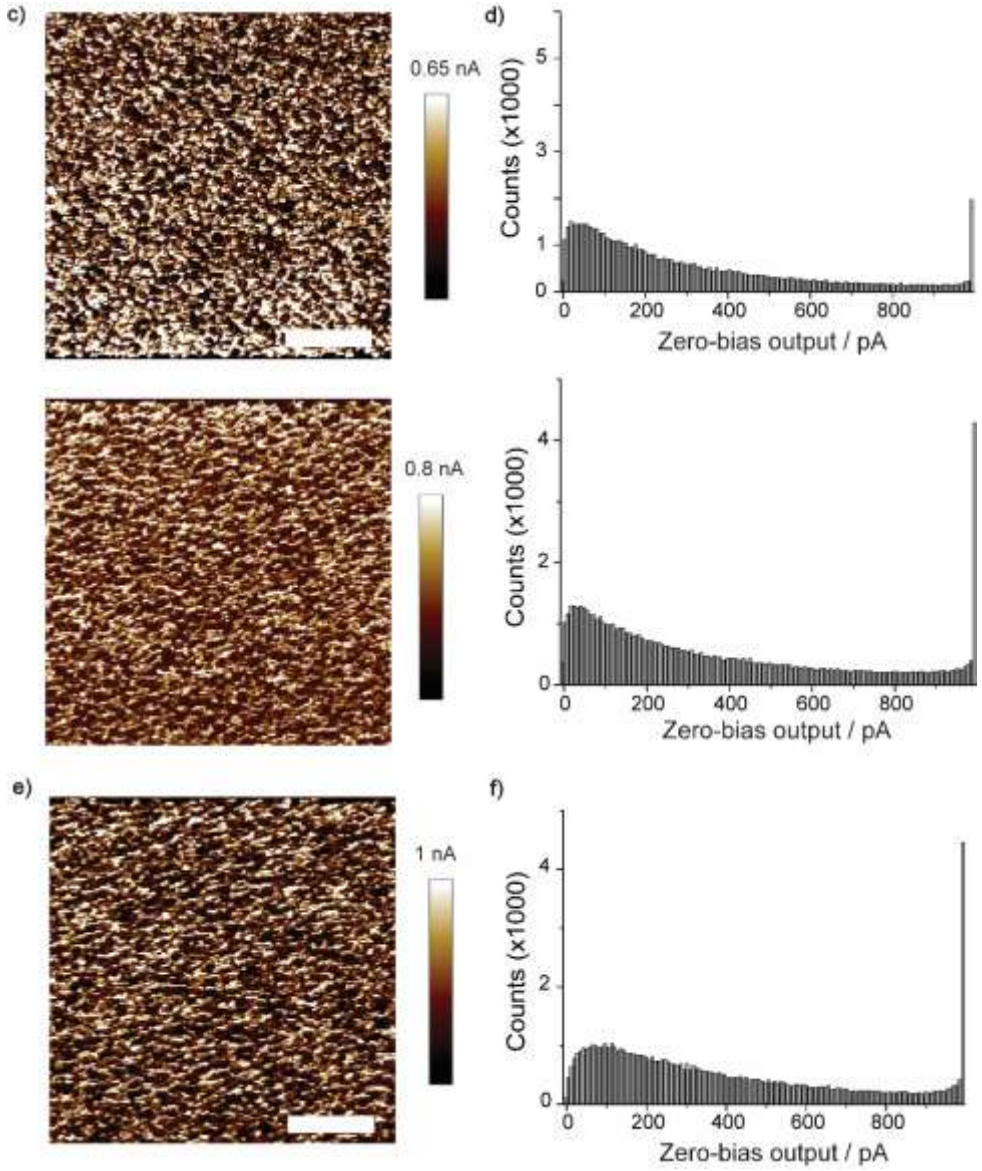

Figure S19. Zero-bias C-AFM maps acquired on **S-1** at different scan rates. Samples were etched under dark for 13 min in a mixture of MeOH and aqueous 40% NH_4F (1:10, v/v). Panels (a, c, e) are current maps recorded at 5 Hz (mean of current value of 295 pA), 7 Hz (mean of current value of 372 pA), and 11 Hz (mean of current value of 397 pA), under 360 nN of normal force. Panels (b, d, f) show histograms of the current output obtained from the C-AFM maps. The histograms y–axis counts indicate the number of pixels (sample locations) of a given current magnitude, with a total of ~65k pixels making up a C-AFM map. Horizontal scale bars in panels (a, c, e) are 1 μm.

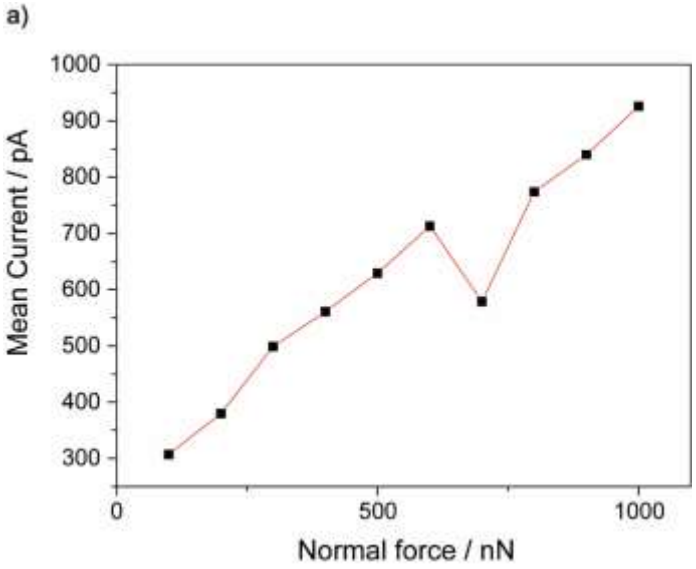

Figure S20. Dependence of the mean zero-bias current output on normal force. Sliding diode C-AFM data obtained on Si(211) **S-1** samples. The substrates were etched for 13 min in a mixture of MeOH and aqueous 40% NH_4F (1:10, v/v) under dark.

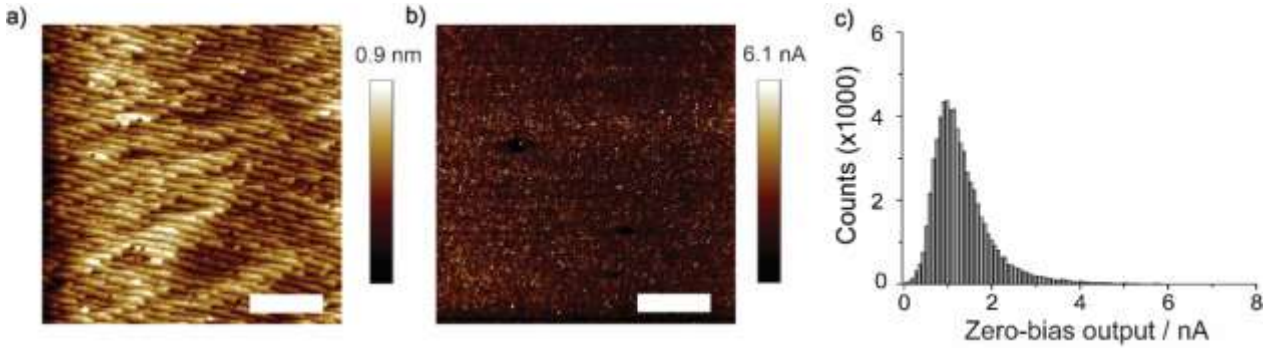

Figure S21. (a) AFM topography image of a **S-2** sample made on Si(111). (b) Zero bias C-AFM map of a **S-2** sample–platinum junction on Si(111). Horizontal scale bars in (a, b) are 1 μm. (c) Histogram plot of the current output of data in (b). Counts indicate the number of pixels of a given current bin, with a total of ~65k pixels being sampled in a single C-AFM map. The current average output was 1.4 nA.

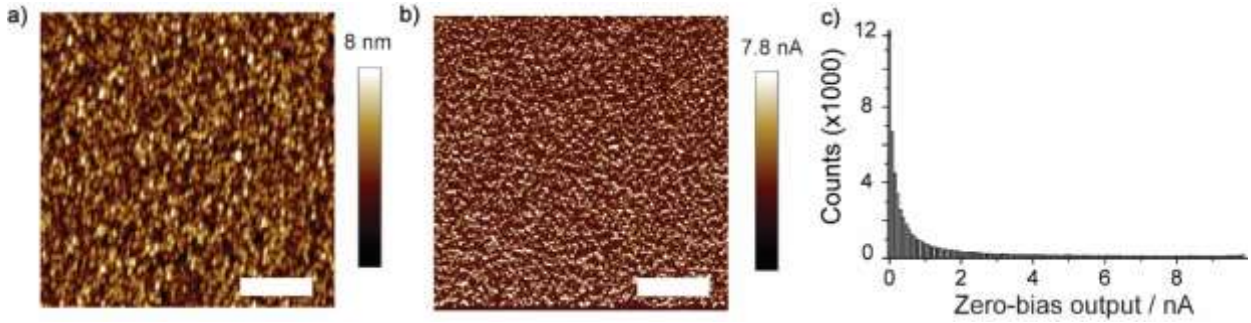

Figure S22. (a) AFM topography image of a **S-2** sample made on Si(211) (b) Zero bias C-AFM map of a **S-2** sample–platinum junction. Horizontal scale bars in (a, b) are 1 μm. (c) Histogram plot of the current output of data in (b). Counts indicate the number of pixels of a given current bin, with a total of ~65k pixels being sampled in a single C-AFM map. Data in figure are for Si(211) wafers etched for 13 min in 1:10 v/v MeOH/NH_4F 40% and shielded from ambient light. The current average average output was 2.3 nA.

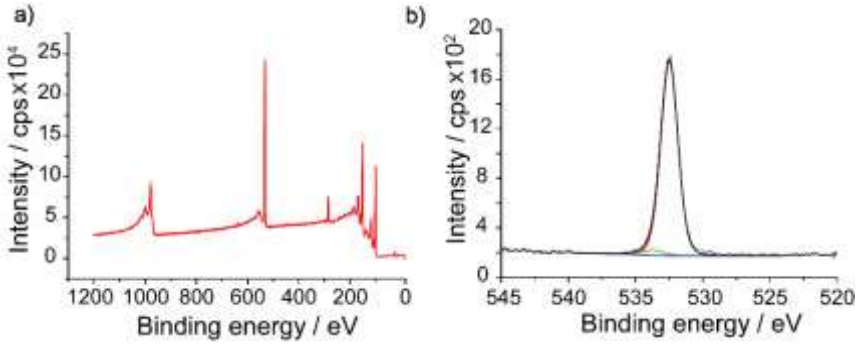

Figure S23. XPS data for **S-1** samples grafted on Si(211). Samples were subjected to 40 CV cycles from −0.4 to 0.6 V, 100 mV/s, 1.0 M $HClO_4$, 1.7 mW cm^{-2} red light electrode illumination. The Si(211) substrates were etched for 13 min in a mixture of MeOH and 40% NH_4F (1:10), shielded from ambient light. (a) XPS survey spectra. (b) Narrow scan of the O 1s region. The spectra were deconvoluted into a main O–Si signal (oxygen bound to Si) at 533 eV, and a second peak signal at higher binding energy attributed to water adsorption to satisfy the fitting.[4]

Section S1

Determination of AFM tip–sample contact area

We estimated the tip–silicon contact area for current density calculations in C-AFM. Calculations were made following the DMT (Derjaguin–Muller–Toporov) model.[5,6]. The contact area is defined by:

$$A = \pi \left\{ \frac{R}{K} (L + 2\pi R\gamma) \right\}^{\frac{2}{3}}$$

Where:

- R is the tip radius,
- *K* is the reduced Young's modulus,

(*K*) is given by:

$$\frac{1}{K} = \frac{4}{3} \left(\frac{1 - \nu_1^2}{E_1} + \frac{1 - \nu_2^2}{E_2} \right)$$

where E is Young's modulus and ν denotes the Poisson ratio. For silicon and platinum Poisson ratios are 0.222 and 0.395, respectively, and the Young's modulus are 162.9 GPa and 177.3 GPa, respectively.[7] The reduced Young's modulus is therefore 70.78 GPa.

- *L* is the Set point (normal applied force)

And $2\pi R\gamma$ is the adhesion force, obtained as the average of 10 force-distance curves. The adhesion force is obtained by averaging data from multiple F–D (force–distance) curves.

Section S2

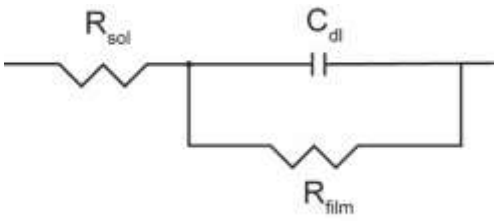

Equivalent electrical circuit used to fit the EIS data acquired at a DC offset (E_{dc}) sufficiently different from ferrocene apparent formal potential. The capacitor was treated as a constant phase element (CPE).

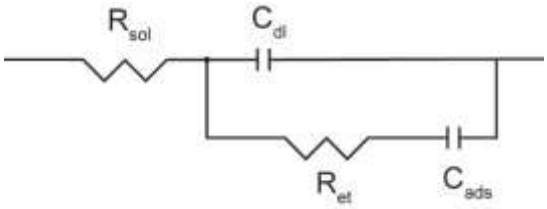

Equivalent electrical circuit used to fit the EIS data acquired at a DC offset (E_{dc}) equal to ferrocene apparent formal potential. Both capacitors were treated as a constant phase element (CPE).

REFERENCES

1. Ciampi, S.; Choudhury, M. H.; Ahmad, S. A. B. A.; Darwish, N.; Brun, A. L.; Gooding, J. J. The impact of surface coverage on the kinetics of electron transfer through redox monolayers on a silicon electrode surface. *Electrochim. Acta.* **2015,** *186*, 216-222.
2. Cerofolini, G. F.; Galati, C.; Renna, L. Accounting for anomalous oxidation states of silicon at the Si/SiO_2 interface. *Surf. Interf. Anal.* **2002,** *33*, 583-590.
3. Scheres, L.; Arafat, A.; Zuilhof, H. Self-Assembly of High-Quality Covalently Bound Organic Monolayers onto Silicon. *Langmuir* **2007,** *23*, 8343-8346.
4. Alam, A. U.; Howlader, M. M. R.; Deen, M. J. Oxygen Plasma and Humidity Dependent Surface Analysis of Silicon, Silicon Dioxide and Glass for Direct Wafer Bonding. *ECS J Solid State Sci. Technol.* **2013,** *2*, 515–523
5. Theiler, P. M.; Ritz, C.; Stemmer, A. Shortcomings of the Derjaguin–Muller–Toporov model in dynamic atomic force microscopy. *J. Appl. Phys.* **2021,** *130*,
6. Park, J. Y.; Salmeron, M. Fundamental aspects of energy dissipation in friction. *Chem. Rev.* **2014,** *114*, 677–711.
7. Hassel Ledbetter, S. K., Monocrystal elastic constants and derived properties of the cubic and the hexagonal elements. In *Handbook of elastic properties of solids, liquids and gases*, M. Levy, H. E. B., R.R. Stern, L. Furr, V. Keppens, Ed. Academic Press.: San Diego, 2001; pp 97–106.